POSITRONIUM REFLECTION AND POSITRONIUM BEAMS

M. Weber,[1] S. Tang,[1] R. Khatri,[1] S. Berko,[2] K.F. Canter,[2] K.G. Lynn,[3]
A.P. Mills, Jr.,[4] L.O. Roellig,[1] and A.J. Viescas[1]

[1] *City College of City University of New York*
[2] *Brandeis University*
[3] *Brookhaven National Laboratory*
[4] *A.T.&T. Bell Laboratories*

Abstract

We have observed specular reflection of positronium, Ps, and established that there is adequate intensity at higher energies to make further study worthwhile. The scattering appears to be restricted to the outermost surface with a mean free path of (0.75 ± 0.15)Å for Ps in LiF(100). With a greater intensity Ps beam one should see higher order diffraction beams as the result of the periodicity of the surface. Ps diffraction thus offers the possibility of being a novel and valuable probe to study the outermost surface and to study adsorbants on it. Two methods for producing Ps beams are described.

Introduction

At the Brookhaven National Laboratory we have initiated a program to study the interaction of positronium, Ps, with the surfaces of solids. An experimental investigation of the reflection of positronium (Ps) from solid surfaces is well warranted because of the fundamental nature of the electronic processes involved in Ps reflection and the possibility of developing a valuable new tool for surface structure determination. Our program of investigating Ps reflection was initiated as a result of the following reasoning. Since Ps can normally be expected to undergo elastic collisions from only the outer atomic layer of a solid, low energy Ps diffraction (LEPSD) could be a unique probe of ordered surface structures. This is somewhat similar to the situation for helium atom diffraction,[1] which is a powerful tool in surface structure determination because it is only sensitive to the outer surface layer. However, the savings in complexity of He atom diffraction by not having to treat multiple scattering from subsurface layers, as in the case of low energy electron diffraction[2-4] (LEED) is somewhat mitigated by having to deal with long range forces that dominate in the diffraction. The $\approx 0.02eV$ energies necessary for He atoms to have ≈ 1Å de Broglie wavelength results in the He atoms having classical turning radii far enough from the individual ion cores that the main scattering is due to the average potential presented by the surface.[1] This requires an accurate treatment of the atom-surface interaction potential which is difficult to obtain and is further complicated because the depth of the van der Waals attractive potential at the surface is approximately the same as the kinetic energy of the helium atom.[5] In order for Ps to have ≈ 1Å de Broglie wavelength, its energy must be on the order of $\approx 75eV$. At this energy, Ps "atoms" would be oblivious to the mean surface potential and only undergo elastic reflection in close encounters with the ion cores. Because of the large break-up probability of Ps (binding energy $= 6.8eV$), multiple scattering and other subsurface contributions to the elastically scattered Ps are expected to be negligible. Thus, Ps diffraction offers the possibility of being a valuable probe.[6]

The degree to which Ps scatters only from the outer surface layer is determined mainly by the interstitial density of valence or conduction electrons of the material. Because of the low mass of weakly-bound electrons, and hence

large recoil, collisions with the electrons destroy the coherence of the scattered Ps and thus must be regarded as a source of attenuation of the incident and diffracted Ps beam. Typical elastic cross sections in the $10eV$ region for Ps-free e^- collisions are on the order of $10^{-15}cm$.[7,8] Thus for solids having interstitial electron densities of $\approx 10^{23}cm^{-3}$,[9-12] a mean free path of ≈ 1Å for the Ps can be expected. Consequently, LEPSD from a solid surface would yield diffracted Ps intensities versus incident energy (i.e., "I(V)" curves) which would be dominated by the elastic scattering from only the outer layer atomic distribution. In the case of an ordered adsorbate overlayer, chemisorbed to a surface, however, the incident Ps could easily penetrate the relatively open spaces between the adsorbate atoms. This would lead to the interesting case of interference between Ps scattering from the adsorbate and from the outer surface with a high sensitivity to the structure of the adsorbate layer and outer surface.

In this paper we will first discuss the results we have already obtained,[13] present an interpretation of them, then provide a description of the method (gas cell) used to produce the Ps beam, and conclude with a description of a completely different method to obtain a Ps beam which is presently under construction.

Positronium Specular Reflection from LiF

Upon entering the experimental chamber the Ps beam divergence is limited by aperture to 5° full width of half maximum of the peak. It is reflected from the sample, S, shown in Fig. 1 and detected by its annihilation gamma rays by two bismuth germanate ($Bi_3Ge_4O_{12}$, titled BGO) detectors in coincidence. The incidence and reflected angles θ_i and θ_r are measured with respect to the normal to the sample; the total angle with respect to the Ps beam is $\psi = \theta_i + \theta_r$. The sample, S, can be rotated through an angle of $50° \leq \theta_i \leq 90°$. The intensity of the detected Ps beam from the gas cell is measured by removing the sample and placing the annihilation plate and BGO detectors at $\psi = 180°$. The distance

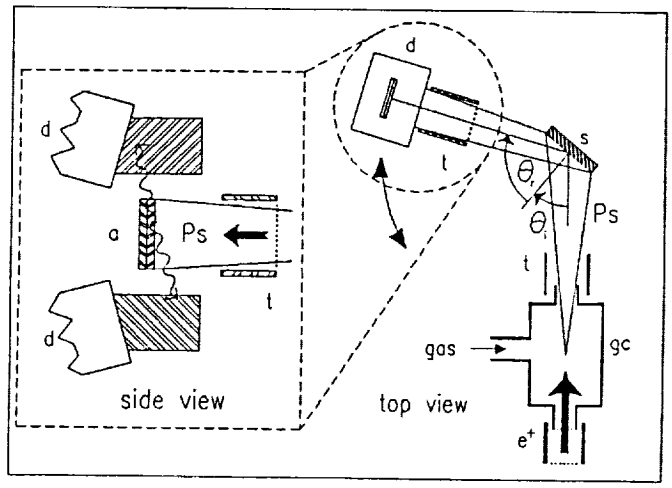

Figure 1 — The experimental arrangement: gc-gas cell, s-sample, t-tubes and grids, and a-annihilation plate.

from the center of the gas cell to the annihilation plate and BGO detectors is a constant, $40cm$, for $100° \leq \psi \leq 180°$. The efficiency for producing and detecting Ps is shown in Fig. 2.

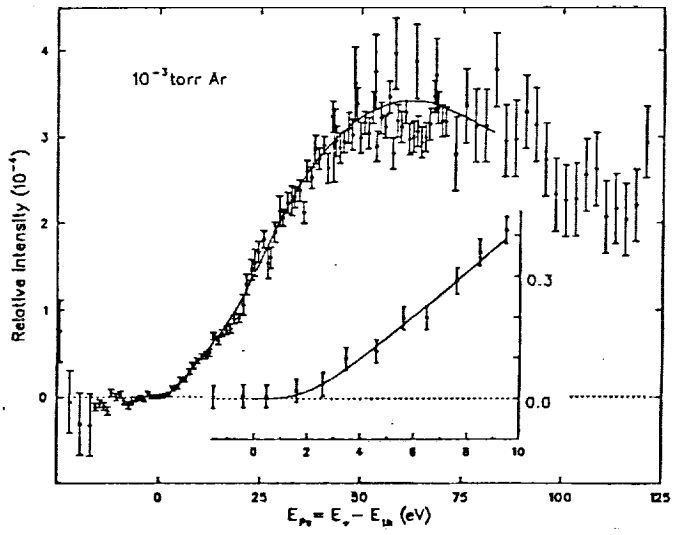

Figure 2 — The efficiency of detecting Ps at the annihilation plate versus the Ps energy. This efficiency was obtained with the gas cell filled with Ar at a pressure of $10^{-3}torr$. The Ps atoms were restricted to a 5° cone (FWHM). The efficiency includes the decay in flight and the Ps detection efficiency.

The efficiency is measured per incident positron versus the Ps energy. It reflects the efficiency of the gas cell filled with $10^{-3} torr$ Ar to form ortho Ps in a 5° cone, the decay in flight of the initial Ps beam, and the ratio of the efficiency to detect of the annihilation gamma rays from Ps to those from positrons. The inset in Fig. 2 is an expanded scale of the low energy Ps region. The absolute efficiency is not required for the measurement of the reflection coefficient because the efficiencies of Ps formation, reflection, and detection are the same (except for 2S Ps) for detecting Ps with the sample removed from the beamline ($\psi = 180°$). We calculate the ratio of the reflected Ps intensity to the intensity at $\psi = 180°$.

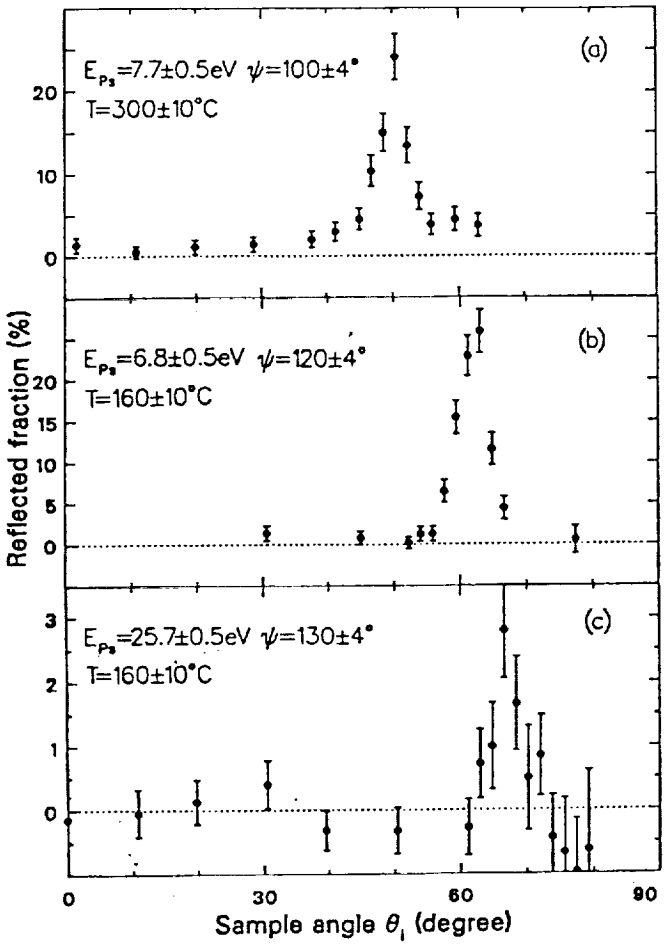

Figure 3 — Reflection probability of Ps at constant incident energy and total scattering angle $\psi = \theta_i + \theta_r$ vs the incident angle, θ_i.

Rocking curves were obtained of the specular reflection of Ps from LiF(100) by rotating the LiF crystal with respect to the Ps beam and holding the detectors fixed. Data was taken with the position of the Ps detector at ψ = 100°, 120°, and 130°. The results for three different Ps energies and three different specular angles are shown in Fig. 3.[13] It is evident the Ps specular reflection does occur and that the reflected fraction is surprisingly high $(30 \pm 5)\%$ at a Ps energy of $7eV$. We also measured the fraction of Ps reflected at a fixed specular angle as a function of the energy of the Ps (see Fig. 4). The fraction of Ps reflected for $\psi = 100 \pm 4°$ from LiF(100) was measured when the LiF was at a temperature of $160 \pm 10°C$ and at a temperature of $300 \pm 10°C$. The two measurements are in good agreement, although the reflection at $300°C$ is somewhat higher than that at $160°C$.

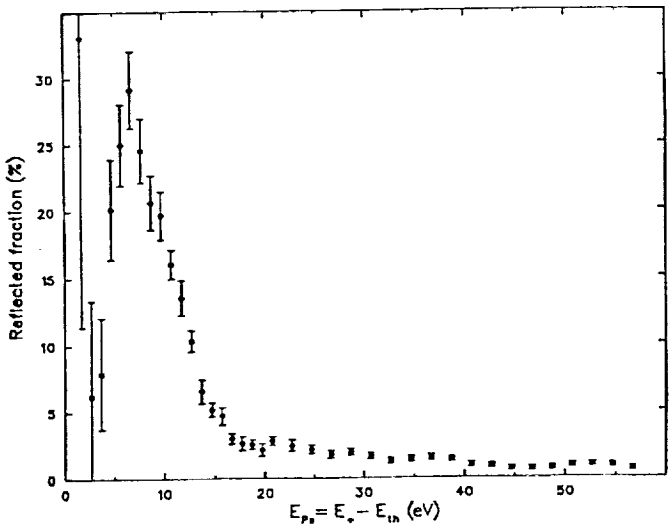

Figure 4 — Ps reflection coefficient as a function of the Ps energy for $\theta_i = \theta_r = 50.4°$.

A simple interpretation of the Ps reflection fraction and its energy dependence can be obtained by considering plane waves reflecting from a potential step. Letting z be the coordinate perpendicular to the crystal surface we consider the potential:
$V(z) = 0$ for $z < 0$, i.e., in the vacuum outside of the crystal; $V(z) = V_r + iV_{im}$ for $z > 0$,

i.e. inside the crystal there is a real and imaginary potential. Using the one dimensional Schrodinger equation in its time independent form we obtain the reflection probability:

$$R = R_o|\frac{k_o - k_{in}}{k_o + k_{in}}| \qquad (1)$$

where k_{in} and k_o are the perpendicular components of the Ps wave vectors inside and outside the crystal, and where the factor R_o is inserted to account for the reflection probability is less than unity at low energies. (This may be due to only a fraction of the surface being clean enough). We estimate $V_r = 4eV$, which is the difference between the binding energy of Ps in the vacuum state ($\approx 7eV$) and the binding energy of Ps inside LiF ($3eV$).[14] If we consider $V_{im} = 0$ and $V_r = 4eV$ we do not predict the observed energy dependence of the reflection probability. R equals R_o for energies less than $V_r/cos^2\theta_i$, but it falls off sharply for higher energies, and finally approaches approximately a $1/E_{P_s}^2$ dependence (see the dashed curve in Fig. 5). Choosing a different V_r only causes a translation of the dashed curve along the horizontal axis, it does not provide a better fit to the data. There is evidently much more apparent elastic scattering than can be accounted for by the real part of the inner potential alone. We can obtain a better fit to the data by adding an energy-dependent imaginary part, V_{im}, to the potential. The wave vector inside the crystal has two components $k_{in} = k_r + ik_{im}$. We can solve Eq. (1) for the value of k_{im} given a certain reflectivity R at a given energy E:

$$k_{im}^2 = \frac{2mE}{\hbar^2} \times \left(\frac{1}{2}\zeta^2[1 + (\frac{1 - 2V_r}{E\zeta^2})^{1/2}] - 1 + \frac{V_r}{2E}\right) \qquad (2)$$
$$\zeta = (R_o + R)/(R_o - R)$$

where $E = E_{P_s}cos^2\theta_i$. By using the data in Fig. 5, with $R = 0.30 \pm 0.05$ and letting $V_r = 4eV$ we can calculate k_{im}. The mean free path is:

$$\lambda = \frac{1}{cos\theta_i}\frac{\int_0^\infty z|\psi|^2 dz}{\int_0^\infty |\psi|^2 dz} = \frac{1}{2k_{im}cos\theta_i} \qquad (3)$$

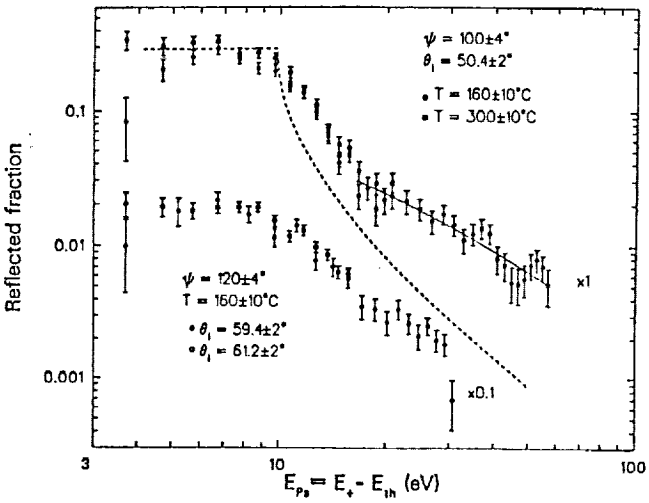

Figure 5 — Ps reflection probability vs the incident Ps energy. The solid line is calculated with the use of Eq. (2) with $V_r = 4eV$ and λ taken from the fitted line in Fig. 6. The dashed line is calculated with $V_r = 4eV$ and $\lambda = \infty$.

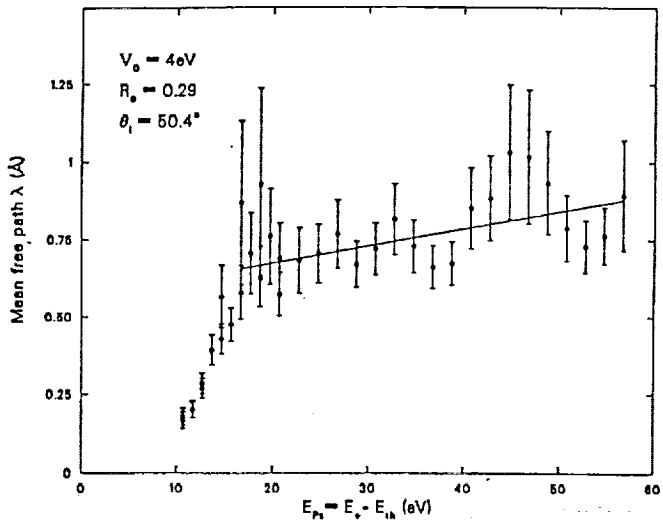

Figure 6 — Ps mean free path calculated from Eq. (2). The straight line is a least-square fit of $\lambda = \lambda_o + aE_{P_s}$ to the data in the interval $16.5eV < E_{P_s} < 56.7eV$. The fitted parameters are $\lambda = (0.57 \pm 0.06)$Å and $a = (4.4 \pm 1.7) \times 10^{-3}$Å$eV^{-1}$, with a χ^2 per degree of freedom $\chi^2/n = 15.26/26$.

where $\psi = Aexp\,(ik_{in}z) = Aexp\,i(k_r + ik_{im})z$. The result plotted in Fig. 6 is $\lambda = (0.75 \pm 0.15)$Å for $16.5eV < E_{P_s} < 56.7eV$. Below $16.5eV$ the mean free path by this analysis becomes unphysically small. The solid line in Fig. 6 is a two parameter fit to the data that suggests λ is slowly increasing with energy. The solid line in Fig. 5 is the corresponding reflectivity calculated with the use of Eq. 2; the dashed line was calculated with a real potential only, i.e. $\lambda = \infty$ and $V_r = 4eV$. The reasonably high-elastic Ps reflection probability observed even at high energies, in spite of the presence of the large absorptive potential is in retrospect not surprising in view of the requirements of unitarity.[15] The reason for the few percent reflection at energies much greater than V_r is principally the short λ. If V_r were to vanish there would still be a measurable reflection coefficient for small λ. In addition one should consider the region between $10eV$ and $16.5eV$ may exhibit a higher reflectivity due to a elastic scattering from the outer most ion cores. It is interesting to note that since the lattice parameter of LiF is 4.02Å, at an incident angle of 50° the first order Bragg diffraction would occur at a Ps energy of $21eV$; however due to the short mean free path at low energies it is hard to envision the high reflectivity would be due to Bragg diffraction at this energy.

It is evident from the above mentioned measurements and analysis that there is a high reflection coefficient and short mean free path for Ps in LiF, and that an intense, well collimated, and monoenergetic Ps beam holds promise as a unique probe of surfaces.

Positronium Beam–Gas Cell Production

Low energy positrons emitted from ^{64}Cu are magnetically transported through an $\vec{E} \times \vec{B}$ filter out of the shielding blockhouse[16] into an Ar gas chamber (see Fig. 7). The pressure of Ar in the gas cell was kept at $10^{-3}torr$. By the use of baffles and by differentially pumping the pressure in the experimental chamber was reduced to $10^{-5}torr$. This relatively high pressure may not have had much effect on the cleanliness of our sample because prior to introducing Ar, which had a purity of 99.995%, into the gas cell; the pressure in the experimental chamber was $10^{-10}torr$. Thus the gas in the experimental chamber was primarily due to Ar from the gas cell. Ps is formed in the gas cell by the positron picking up an electron from the Ar atom.[17–19] The ionization potential for Ar is $15.8eV$, however, the binding energy of Ps is $6.8eV$ thus the threshold energy for Ps production is a positron energy of $9.0eV$. The first excited state of the Ar atom is $11.5eV$ and the first excited state of Ps is $5.1eV$ above the ground state. Thus a positron beam which an energy between $9.0eV$ and $14.1eV$ will produce a monoenergetic beam of Ps in the energy range of $0 - 5.1eV$. The ratio of the cross section for e^+ to produce Ps in the 2S state to producing Ps in the 1S state reaches its maximum value of 13% for an e^+ energy of $50eV$ in He.[20](We are unaware of any calculations for a similar ratio in Ar). Above $20.5eV$ it is energetically possible to produce Ps after exciting an Ar atom. However, the probability of a positron undergoing both collisions in the gas cell is exceedingly low. In summary, we estimate that the excited state contamination of our beam to average less than 5% and the energy purity due to Ar excitation to be less than 1%.

Positronium Beam–Foil Production

We are presently constructing a new high intensity positron beam in the Material Science Building across the street from the High Flux Beam Reactor (HFBR) Building. The new facility will have four advantages over the present one located at the reactor: the low energy positron beam will be more intense than the beam used for our first generation Ps experiment described here; we will not be subject to the increasingly more severe security regulations which exist on the operating level of the HFBR; the background radiation will be greatly reduced; and the area available for experiments will be increased. The new facility will have a blockhouse approximately twice the size of the one built in the reactor building. It is planned

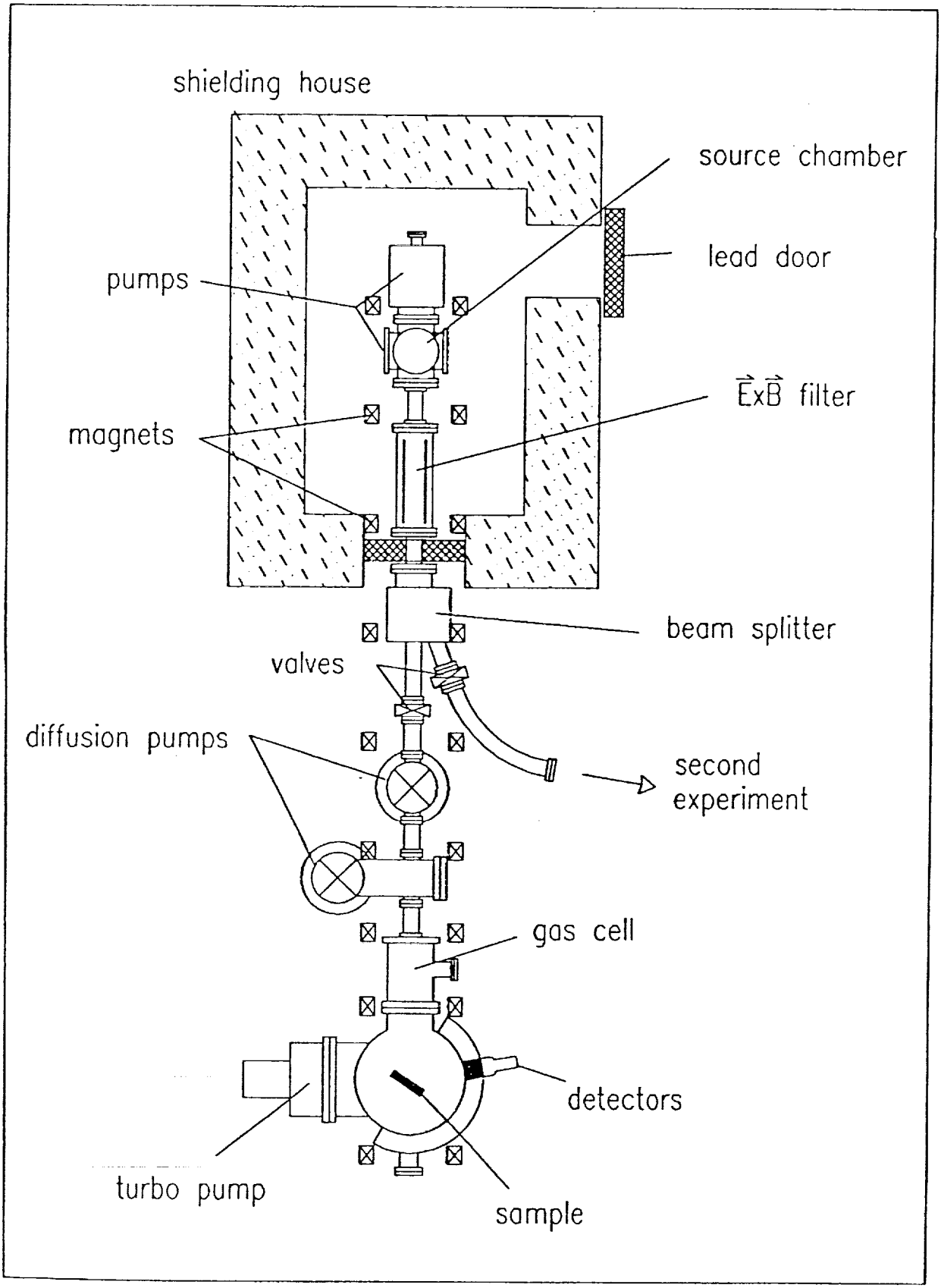

Figure 7 — Schematic view of the apparatus to produce a positron beam and a Ps beam by the gas cell method.

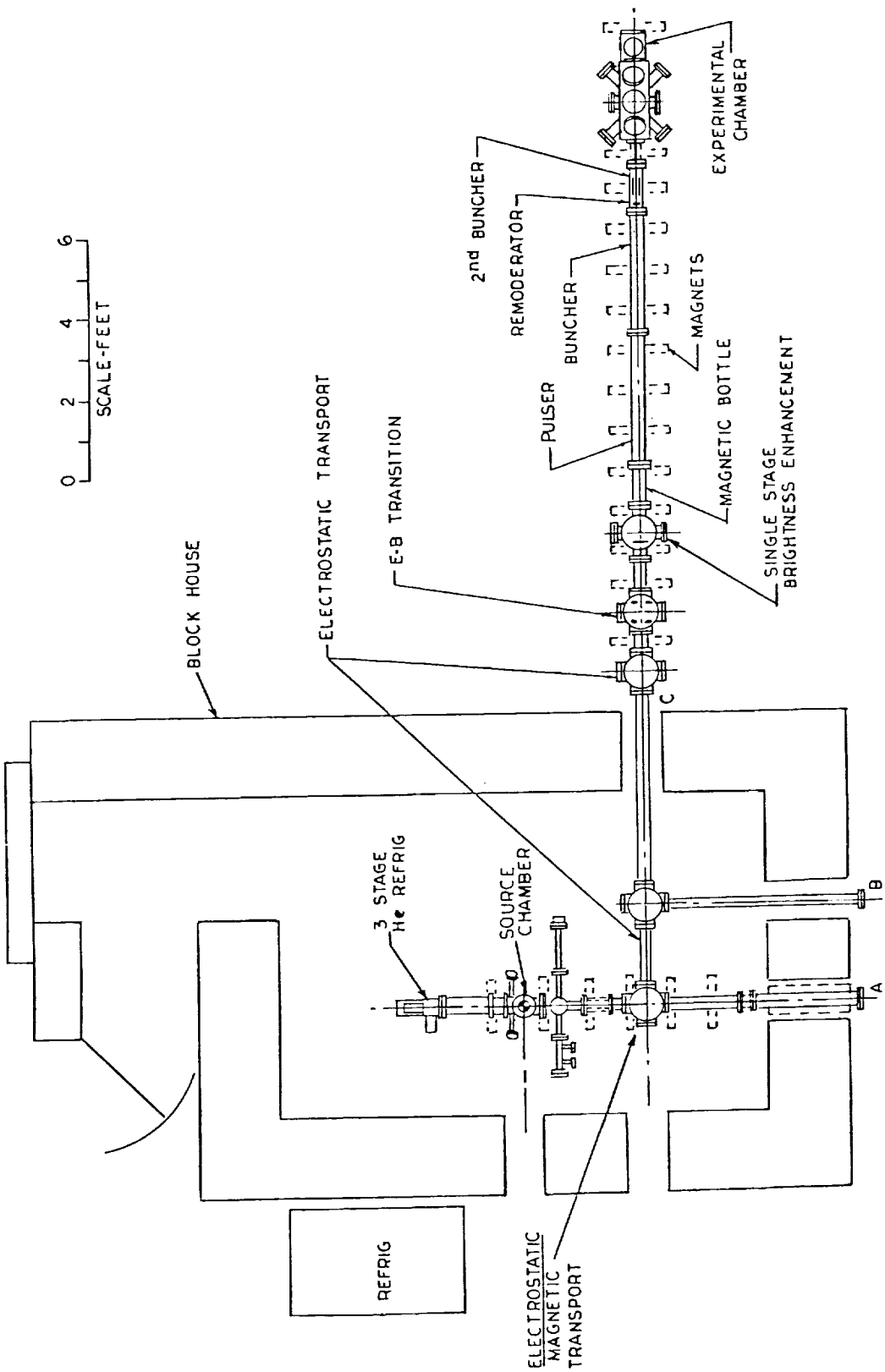

Figure 8 — Schematic view of the apparatus to produce a positron beam and a Ps beam by the foil method.

to have three low energy positron beam ports, the present blockhouse has one beam port. Two ports (ports B and C in Fig. 8) will have a electrostatic transport system and the third (port A) will be a magnetically guided transport system. A copper pellet will be irradiated in the core of the HFBR for 2 days, then removed from its capsule in a blockhouse located alongside of the reactor on the operations level of the HFBR and deposited into a lead and heavi-met container. It will then be transported by an electric truck to the Material Science Building, and inserted into a crucible in the new blockhouse. The copper pellet will be evaporated onto the inside of a cone which then will have deposited on it 10^4Å of solid Ne. Our past moderator was crystalline copper, but our future one will be solid neon because of its higher efficiency. We have measured an efficiency of $\approx 1\%$ for producing low energy positrons with solid neon in a cone configuration.[21-24]

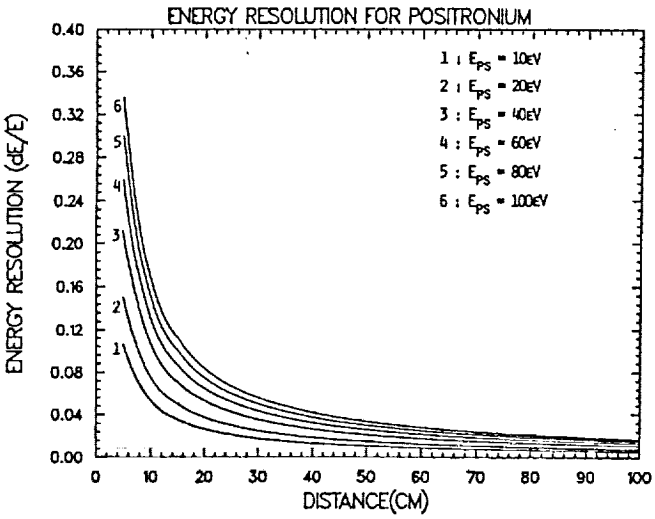

Figure 9 — The energy resolution for observing Ps in a pulse of $8ns$ width vs distance from the foil to the detector for various Ps energies.

Instead of using the charge transfer of an electron from the Ar atom to combine with a positron to produce Ps we will send positrons through a thin carbon foil to produce them.[25] The positron beam will be pulsed which allows us to perform time of flight measurements. This method has three distinct advantages in comparison to the gas cell method to produce Ps. The advantages are first the surface of the sample will not be as easily subject to contamination as it is from the gas cell since we will be able to operate in a $\approx 10^{-10} torr$ environment. The second advantage is that we will be able to have a direct measure of the energy of each Ps atom with better resolution. Third, although the Ps produced by the foil would not be as monoenergetic as can be obtained using a rare gas target the time of flight method would give us the advantage of being able to investigate many energies at once.

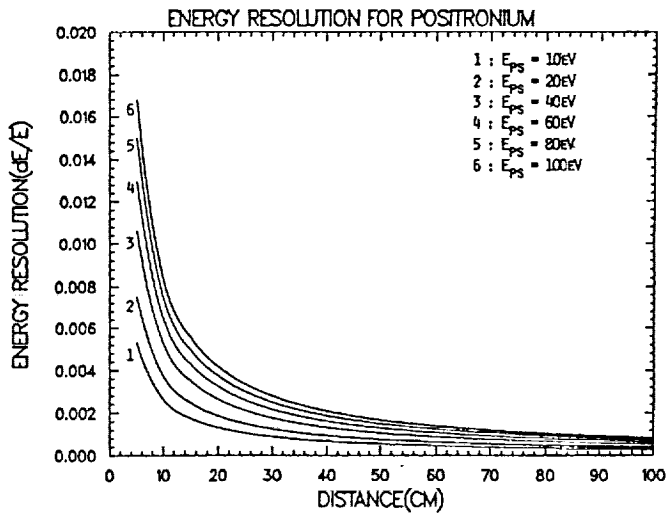

Figure 10 — The energy resolution for observing Ps in a pulse of $0.1ns$ width vs distance from the foil to the detector for various Ps energies.

The new Ps beam will be produced by the following method.[26,27] The positron beam will be transported out of the blockhouse electrostatically. It will then enter a magnetically guided section. It is then remoderated to minimize its transverse energy component and injected into a pinched magnetic field to enter a magnetic bottle. Upon entering the bottle the beam transverses a rf cavity which oscillates at 430MHz to give it transverse motion and to excite the positron cyclotron resonance. The positrons are then reflected by a positive potential on a grid, they again transverse the

rf cavity and they now have enough transverse motion to be reflected by the pinched magnetic field at the entrance of the bottle. The positrons now oscillate between the two ends of the trap for $100\mu s$. During this time positrons continue to stream into the trap from the radioactive source and accumulate in the trap. After a $100\mu s$, the grid which was at a positive potential is given a negative potential pulse by an oscillator operating at 10kHz and the positrons enter a section of 100 ring electrodes each having a bias such that the accumulated positrons experience a potential which varies harmonically with distance along the beamline and are bunched to a pulse of width $8ns$. The total length of the accumulator/pulser/buncher is $90inches$. This accumulator/pulser/buncher has been constructed, tested and measured to have an efficiency of 63%.[26] Upon leaving the buncher the positrons are again remoderated and enter a second buncher of length one inch which produces a harmonic potential due to a geometric distortion of the electric field at one end of the buncher. This second buncher will reduce the positron pulse width from $8ns$ to a subnanosecond bunched positron beam. The technical details of the first accumulator/pulser/buncher are given in Refs. 26 and 27 and the details of the second buncher are given in Ref. 28. Upon leaving the second buncher, the positrons traverse a carbon foil and produce a pulsed beam of Ps atoms which then enter the experimental chamber which was described above. The charged particles in the beam are removed by electric fields. The energy of the Ps atom is determined by measuring the time difference between the time the pulsed positron beam strikes the carbon foil and the time the positronium atoms travel a fixed distance to the Ps detection system. The pulse width of the positrons leaving the buncher very much affects the measured energy resolution of the Ps atom. This is shown in Figs. 9 and 10 which plot the Ps energy resolution versus Ps flight path for various energies of the Ps atom. Fig. 9 is for a positron pulse width of $8ns$ and Fig. 10 is for a positron pulse width of $0.1ns$. Although a longer flight path increases the energy resolution it also reduces the number of Ps atoms detected due to Ps decay. The effect of Ps decay in flight is given in Fig. 11 which plots the Ps attenuation coefficient as a function of Ps energy for various length of flight paths.

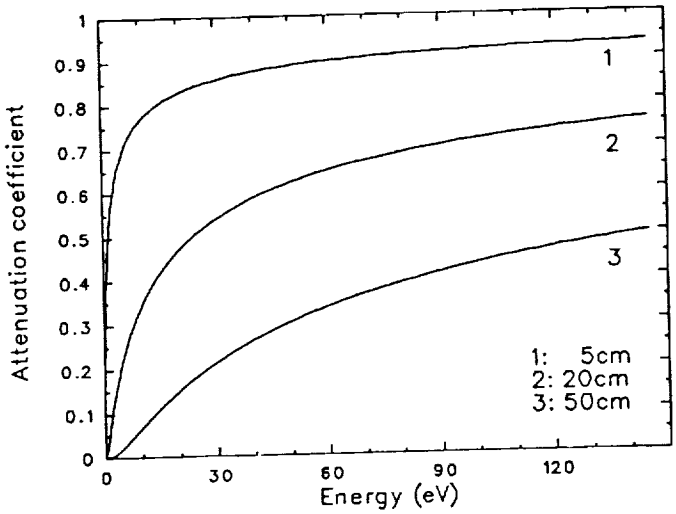

Figure 11 — The attenuation coefficient for Ps decay in flight vs the Ps energy for various flight path distances.

The table below shows the expected efficiencies of the various components of the pulsed Ps beam production. The average efficiency was calculated for the production of Ps in the energy range of $6eV$ to $100eV$ in a solid angle of 10^{-2} steradian after traveling a path length of $20cm$. The column at the right lists the number of particles to be expected at each stage of the beamline. These numbers are predicated on a spherical copper pellet of weight of $0.86g$ and diameter $0.57cm$ placed in the core of the HFBR for a period of 48 hours where the positron-emitting isotope ^{64}Cu is produced by the reaction ^{63}Cu(n,γ) ^{64}Cu. The activity of the pellet after 48 hours is $100.5Ci$ of positron emission.[16] Our past experience indicates that approximately one-third of this activity can be evaporated unto a surface because of losses due to decay during the time period from removing the source from the reactor to completing the evaporation of the Cu on a surface, and due to Cu vapor escaping and not being deposited on

the surface. We have obtained a moderating efficiency of 1.2% with a solid Ne moderator,[24] but for the purpose of these calculations we are estimating an efficiency of 0.7%. We expect the efficiency of the 90° bender in the blockhouse to be 90%. The number of low energy positrons entering the remoderator given in the table, $7.8 \times 10^9 sec$, results from these calculations. It is the number of particles during the beginning of a run, for ^{64}Cu decays with a half-life of 12.8 hours. At the end of a two day run the number will be reduced by a factor of ≈ 16.

Ps BEAM EFFICIENCY

Process	Efficiency in %	Number of Particles e^+/sec
Slow positrons into remoderator		7.8×10^9
Remoderator 1	30	2.3×10^9
Accumulator/pulser/buncher	63	1.4×10^9
Remoderator 2	30	4.2×10^8
Ps formation in foil *)	8.9×10^{-3}	3.7×10^4
Loss in three grids †)	72	2.7×10^4

*) energy range $6eV$ to $100eV$ in a solid angle of $10^{-2} ster.$ after traveling a path length of $20cm$.[25]
†) 90% transmission grids

An extensive research program is planned to vary the parameters of the carbon foil to improve its efficiency to produce Ps (foil thickness, positron energy, coatings on foil, other foils etc.). Another consideration which will be examined is the effect of a $34Ci$ of positron emission source on the Ne moderator. Will it cause the surface to be charged? Will it produce a large number of defects in the solid Ne? Both effects could adversely effect its efficiency. In the event that Ne moderation is adversely affected by a strong radioactive source we plan to revert back to a transmission moderator to produce low energy positrons and to compensate for its lower efficiency by using a stronger ^{64}Cu source.

Summary

Positronium reflection from a surface shows promise to be an extremely sensitive surface probe. We have shown that the mean free path in LiF(100) of Ps atoms in the energy range $16.5eV < E < 56.7eV$ is 0.75 ± 0.15Å.[13] This assures us that analysis of Ps diffracted intensities will only have to take into account the outer most atomic layer, and thus avoids the complication encountered in LEED where the mean free path is typically an order of magnitude larger.[29]

A description is given of two different methods for producing a Ps beam. Each method has its own set of advantages. The gas cell method will produce a monoenergetic Ps beam at low energies, whereas the foil beam will allow the sample to be in an ultra high vacuum environment and the energy of each Ps atom can be measured by a time of flight technique. The work was supported in part by the National Science Foundation (Grant No. DMR-8620168), and in part by the Division of Material Sciences, U.S. Department of Energy, under contract No. DE-AC-76CH0016.

References:

1. K.H. Rieder and N. Garcia, *Phys. Rev. Lett.* **49**, 43 (1982).

2. See, for example, F. Jona, *J. Phys. C* **11**, 4271 (1978).

3. C.B. Duke, in *Surface Properties of Electronic Materials*, edited by D.A. King and D.P. Woodruff (Elsevier, New York, 1986), Chap. 3.

4. A. Kahn, *Surf. Sci. Rep.* 4/5, 193 (1983).

5. H. Hoinkens, *Rev. Mod. Phys.* **52**, 933 (1980).

6. K.F. Canter, in *Positron Scattering in Gases*, edited by J.W. Humberston and M.R.C. McDowell (Plenum, New York, 1984), p. 219.

7. S.J. Ward, J.W. Humberston, and M.R.C. McDowell, *J. Phys.* B: At. Mol. Phys. **18**, L525 (1985).

8. S.J. Ward, J.W. Humberston, and M.R.C. McDowell, *J. Phys.* B: At. Mol. Phys. **20**, 127 (1987).

9. P.J.E. Alfred and M. Hart, *Proc. R. Soc. Lond.* **A 332**, 239 (1973).

10. J.A. Golovchenko, D.E. Cox, and A.N. Goland, *Phys. Rev.* **B 26**, 2335 (1982).

11. B. Dawson, *Proc. R. Soc. Lond.* **A 298**, 395 (1967).

12. A.J. Freeman, in *Electron and Magnetization Densities in Molecules and Crystals*, edited by P. Becker (Plenum Press, New York and London, 1980) p. 83.

13. M. Weber, S. Tang, S. Berko, B.L. Brown, K.F. Canter, K.G. Lynn, A.P. Mills, Jr., L.O. Roellig, and A.J. Viescas, *Phys. Rev. Lett.* **61**, 2542 (1988).

14. A. Dupasquier, in *Positron Solid State Physics*, edited by W. Brandt, A. Dupasquier (North-Holland, Amsterdam, 1983), p. 510.

15. Unitarity requires inelastic scattering to be accompanied by elastic scattering: see, for example, P. Roman, *Advanced Quantum Theory* (Addison-Wesley, Reading, MA, 1965), p. 198.

16. K.G. Lynn, A.P. Mills, Jr., L.O. Roellig, and M. Weber, in *Electronic and Atomic Collisions* , edited by D.C. Lorents, W.E. Meyerhof, and J.R. Peterson (North-Holland, Amsterdam, 1986) p. 227.

17. L.O. Roellig, M. Weber, S. Berko, B.L. Brown, K.F. Canter, K.G. Lynn, A.P. Mills, Jr., S. Tang, and A. Viescas, in *Atomic Physics with Positrons*, edited by J.W. Humberston and E.A.G. Armour (Plenum, New York, 1987), p. 233.

18. G. Laricchia, S.A. Davies, M. Charlton, and T.C. Griffith, *J. Phys.* E: Sci. Instrum. 21, 886 (1988).

19. B.L. Brown, in *Positron (Electron)-Gas Scattering*, edited by W.E. Kauppila, T.S. Stein, and J.M. Wadehra (World Scientific Publishing Co. Pte Ltd., Singapore, 1986) p. 212.

20. P. Khan, P.S. Mazumdar, A.S. Ghosh, *J. Phys.* B: At. Mol. Phys. **17**, 4785 (1984).

21. K.G. Lynn, E. Gramsch, S.G. Usmar, and P. Sferlazzo, *Appl. Phys. Lett.* **55**, 87 (1989).

22. A.P. Mills, Jr., and E.M. Gullikson, *Appl. Phys. Lett.* **49**, 1121 (1986).

23. E.M. Gullikson and A.P. Mills, Jr., *Phys. Rev. Lett.* **57**, 376 (1986).

24. R. Khatri, M. Charlton, P. Sferlazzo, K.G. Lynn, and A.P. Mills, Jr., (unpublished) 1988.

25. A.P. Mills, Jr. and W.S. Crane, *Phys. Rev.* **A 31**, 593 (1985).

26. A.P. Mills, Jr., E.D. Shaw, R.J. Chichester, and D.M. Zuckerman, *Rev. Sci. Instrum.* **60**, 825 (1989).

27. A.P. Mills, Jr., *Appl. Phys.* **22**, 273 (1980).

28. W.S. Crane, and A.P. Mills, Jr., *Rev. Sci. Instrum.* **56**, 1723 (1985).

29. M.G. Lagally, in *Methods of Experimental Physics*, Vol. 22, edited by R.L. Park and M.G. Lagally (Academic Press, Inc., Orlando 1985) p. 237.